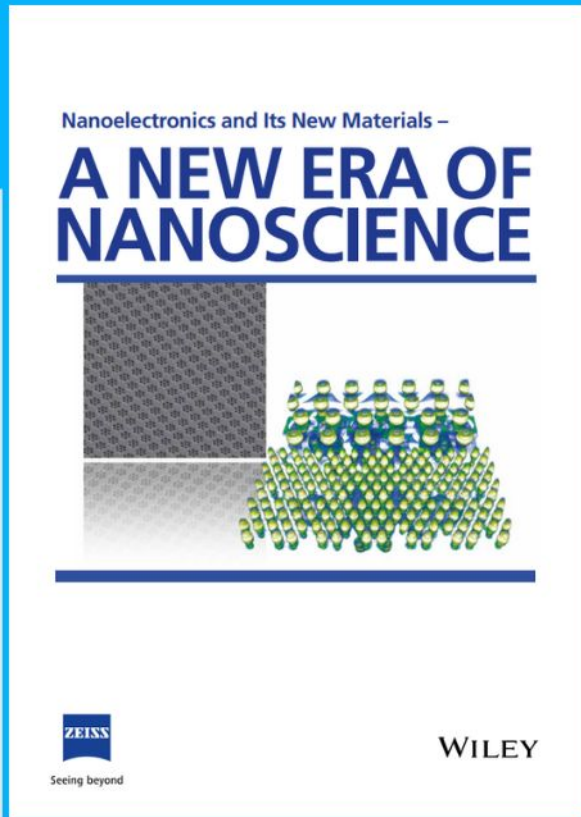




Nanoelectronics and Its New Materials – A NEW ERA OF NANOSCIENCE



Discover the recent advances in electronics research and fundamental nanoscience.

Nanotechnology has become the driving force behind breakthroughs in engineering, materials science, physics, chemistry, and biological sciences. In this compendium, we delve into a wide range of novel applications that highlight recent advances in electronics research and fundamental nanoscience. From surface analysis and defect detection to tailored optical functionality and transparent nanowire electrodes, this eBook covers key topics that will revolutionize the future of electronics.

To get your hands on this valuable resource and unleash the power of nanotechnology, simply download the eBook now. Stay ahead of the curve and embrace the future of electronics with nanoscience as your guide.



Seeing beyond

WILEY

Anti-Tumor Immunity Induced by a Ternary Membrane System Derived From Cancer Cells, Dendritic Cells, and Bacteria

He Ren, Jiexin Li, Jingyu Zhang, Jingang Liu, Xingyue Yang, Nan Zhang, Qian Qiu, Dan Li, Yue Yu, Xiaofeng Liu, Jonathan F. Lovell, and Yumiao Zhang*

Cancer vaccines generally are limited by insufficient tumor-specific cellular immunogenicity. Herein, a potent “ABC” ternary membrane-derived vaccine system blended from antigen-presenting mature dendritic cell membranes (“A”), bacterial *E. coli* cytoplasmic membranes (“B”), and cancer cell membranes (“C”) is developed using a block-copolymer micelle-enabled approach. The respective ABC membrane components provide for a source of cellular immune communication/activation and enhanced accumulation in lymph nodes (A), immunological adjuvant (B), and tumor antigens (C). The introduction of dendritic cell (DC) membranes enables multiple cell-to-cell communication and powerful immune activation. ABC activates dendritic cells and promotes T-cell activation and proliferation *in vitro*. *In vivo*, ABC is 14- and 304-fold more immunogenic than binary (BC) and single (C) membrane vaccines, and immunization with ABC enhances the frequency of tumor-specific cytotoxic T lymphocytes, leading to an 80% cure rate in tumor-bearing mice. In a surgical resection and recurrence model, ABC prevents recurrence with vaccination from autologous cancer membranes, and therapeutic effects are observed in a lung metastasis model even with heterologous cancer cell membranes. ABCs formed from human cancer patient-derived tumor cells activate human monocyte-derived dendritic cells (moDC). Taken together, the ternary ABC membrane system provides the needed functional components for personalized cancer immunotherapy.

stimulate dendritic cell activation and subsequently can promote the activation and proliferation of downstream specific cytotoxic T cells to achieve the inhibition or elimination of solid tumor progression.^[4–6] For specific cellular immune activation, vaccines frequently involve the co-delivery of tumor characteristic antigenic peptides and adjuvants, while clinical therapeutic efficacy is usually impeded by lack of vaccine immunogenicity as well as tumor immunosuppression and heterogeneity.^[3,7,8] In addition, tumor cells express limited or no immunogenic antigens, resulting in immune evasion.^[9] Biomimetic nanomaterials have diverse and unique physiological functions after evolution, which are difficult to recreate by synthetic materials.^[10–12] Biological complexes displayed on the membrane of different types of cells endow them specific properties.^[13,14] Autologous cancer vaccines involving use of membranes from cancer as a wide spectrum source of natural tumor antigens have spurred great interest.^[15] B16F10 cancer membrane has been coated on PLGA nanoparticles, leading to matured dendritic cells and prolonged survival in tumor-bearing mice.^[16]

1. Introduction

Immunotherapy using cancer vaccines has shown promise in the clinical treatment of a variety of cancers.^[1–3] Vaccines

Similar studies were also conducted to use membranes of B16 or MDA-MB-231 cells to achieve strong immunostimulatory responses.^[17,18] Compared to specific antigens loaded in vaccines, membrane-derived biomaterials with natural antigens

H. Ren, J. Li, J. Zhang, J. Liu, N. Zhang, Q. Qiu, Y. Zhang
School of Chemical Engineering and Technology
Key Laboratory of Systems Bioengineering (Ministry of Education)
Tianjin University
Tianjin 300350, P. R. China
E-mail: ymzhang88@tju.edu.cn
X. Yang
School of Life Science and Technology
Weifang Medical University
Shandong 261000, P. R. China

D. Li, Y. Yu, X. Liu
The First Department of Breast Cancer
Tianjin Medical University Cancer Institute and Hospital
Key Laboratory of Breast Cancer Prevention and Therapy
Ministry of Education
Key Laboratory of Cancer Prevention and Therapy
National Clinical Research Center for Cancer
Tianjin 300060, P. R. China
J. F. Lovell
Department of Biomedical Engineering
State University of New York at Buffalo
Buffalo, NY 14260, USA

 The ORCID identification number(s) for the author(s) of this article can be found under <https://doi.org/10.1002/sml.202302756>

DOI: 10.1002/sml.202302756

have more flexibility for personalized vaccines.

As bacterial components such as proteins, lipids and nucleic acids can stimulate immune system, vaccines using bacterial cell membrane coatings have been prepared for the prevention and treatment of bacterial infections, virus invasion and cancer production.^[19] A meningococcal vaccine has been currently in clinical use containing meningococcal group B outer membrane.^[20] Nanoparticles coated by whole *S. flexneri* outer membrane vesicles are also shown to induce a higher level of protection against bacterial challenge.^[21] Recently, bacterial outer membranes have been verified to be effective candidates for enhanced specific antitumor responses by inducing adaptive immune response.^[22,23] Pathogen-associated molecular patterns (PAMPs) present on bacterial membranes and antigens present on tumor membranes could be incorporated in nanovaccines for the prevention of tumor recurrence after surgery.^[24] Bacterial membrane fractions provide abundant immune signals to trigger corresponding innate and adaptive immunity, activating the immune system in a manner similar to infection signals.

In addition, introduction of specific immune cell membranes associated with important immune process could facilitate cross-priming and rapid activation of systemic immune responses.^[25] Membrane of natural killer cells cloaked photosensitizer was used for the combination therapy of photodynamic therapy and immunotherapy.^[26] Also, dendritic cell-derived co-stimulatory markers (CD80) were engineered to be expressed in a tumor cell line and the membrane from these engineered cells was used to prepare nanovaccines to enable presentation antigens in an immunostimulatory context.^[27] As an important component of adaptive immunity, the abundance of co-stimulatory molecules and major histocompatibility complexes (MHCs) on membranes stimulate T cells directly, resulting in efficient tumor resistance against targeted antigens. Hybrid dendritic cell (DC) and tumor membrane coated nanoparticles promotes systemic specific immunity for distal tumor elimination in combination with photothermal treatment.^[25] In spite of having some similar immune functions as bacterial membrane such as DC activation, DC membranes have their own unique functions such as communication with immune cells such as T cells and enhanced accumulation in lymph nodes.

Taking the aforementioned points together, herein, we separated B16 tumor cells membranes, *E. coli* cytoplasmic membranes and mature DC membranes and prepared ternary membrane nanovaccines by co-extrusion. B16 tumor cells membranes provide a broad spectrum of cancer antigens; *E. coli* cytoplasmic membranes contain PAMPs that could activate immune system as adjuvants; DC cell membranes can increase the accumulation in lymph node and interaction with immune cells such as T cells. This ternary membrane nanovaccine effectively primes the maturation of DCs and promotes the proliferation of specific cytotoxic T cells in vivo, resulting in the regression of tumors.

2. Results and Discussion

2.1. Nanovaccine Characterization

To prepare ternary membrane cloaked nanovaccines, membranes of tumor cells, bacterial cytoplasmic and dendritic cells were collected and coated successively onto F127 micelles as il-

lustrated in **Figure 1**. Membranes from tumor cells contain both tumor specific antigens (TSAs) and tumor associate antigens (TAAs) as previously reported.^[28,29] The results of LC-MS (Table S1, Supporting Information) for membrane proteins illustrate that B16 cancer cell membranes contain multiple MHC complexes and specific immunogenic B16 mutations such as Actn4, Eef2 and Rpl13a.^[30] Membrane from bacterial cytoplasmic membranes contain immunomodulating molecules like TLR ligands, that could act as adjuvants as shown in Table S2, Supporting Information. Cell membranes from bacteria including *S. aureus*, *B. subtilis* and *E. coli* Nissle 1917 were screened and no significant difference or synergistic effect was found in their ability to activate dendritic cells as adjuvants (Figure S1, Supporting Information). We selected membranes of *E. coli* Nissle 1917 as adjuvants, which is a well-studied probiotic with a long track of safety in humans.^[31] Membranes from mature dendritic cells were used as the third component, containing co-stimulatory molecules (Figure S2, Supporting Information). Other characteristic proteins on mature DC cell membranes such as CD14, CD47, and CD84 possess the ability to directly activate T cells and modulate innate immunity in response to bacterial infections (Table S3, Supporting Information).^[32–34] We hypothesize that its introduction could confer the vaccine the ability to communicate with multiple immune cells simultaneously, achieving further immune enhancement. 5,9,14,18,23,27,32,36-Octabutyoxy-2,3-naphthalocyanine (ONc) loaded F127 micelles were prepared and used as a scaffold for membrane coating, which could be potentially used as a contrast agent for bioimaging to track nanovaccine delivery (but not investigated in this study). Nanovaccines containing single (cancer cell membrane alone), binary (bacterial membrane and cancer cell membrane)- or ternary membranes (antigen-presenting DC membrane, bacterial membrane and cancer cell membrane) were prepared separately by coextrusion with ONc-encapsulated F127 micelles, and they are referred to as C, BC, and ABC, respectively. To optimize the ratio of each membrane in the nanovaccine, different formulations were screened by co-incubation with DC cells, followed by the examination of levels of co-stimulatory molecule expression, pro-inflammatory cytokine secretion and antigen presentation. As shown in Figures S3 and S4, Supporting Information, the percentage of mature DC cells after stimulation reached 51.9% and the secretion of inflammatory cytokines IL-6 and IL-12 almost remained unchanged with the increase of the ratio of cell membrane to micelles, so the mass ratio of membrane protein and micelle of 1:1 was chosen. With the same total amount of membrane proteins added, different ratios of A and B were investigated and the ratio of 1:1 was also selected for the A and B fractions (Figures S5 and S6, Supporting Information). With the ratio of A:B as 1:1, the effects of different addition ratios of C were studied by examining the DC cell maturation, cytokine secretion and antigen presentation (Figures S7–S9, Supporting Information). Therefore, the final mass ratio of 1:1:1 (A:B:C) was chosen in the final ABC nanovaccine.

Transmission electron microscopic (TEM) images showed that the size of ABC nanovaccines were ≈ 100 nm (**Figure 2a**). The size of C, BC, ABC nanovaccine were all about 100–200 nm and ABC vaccine had a size of 130 nm measured by dynamic light scattering (DLS) analysis (**Figure 2b**). The negative charge on the surface of the vaccines gradually increased with the successive

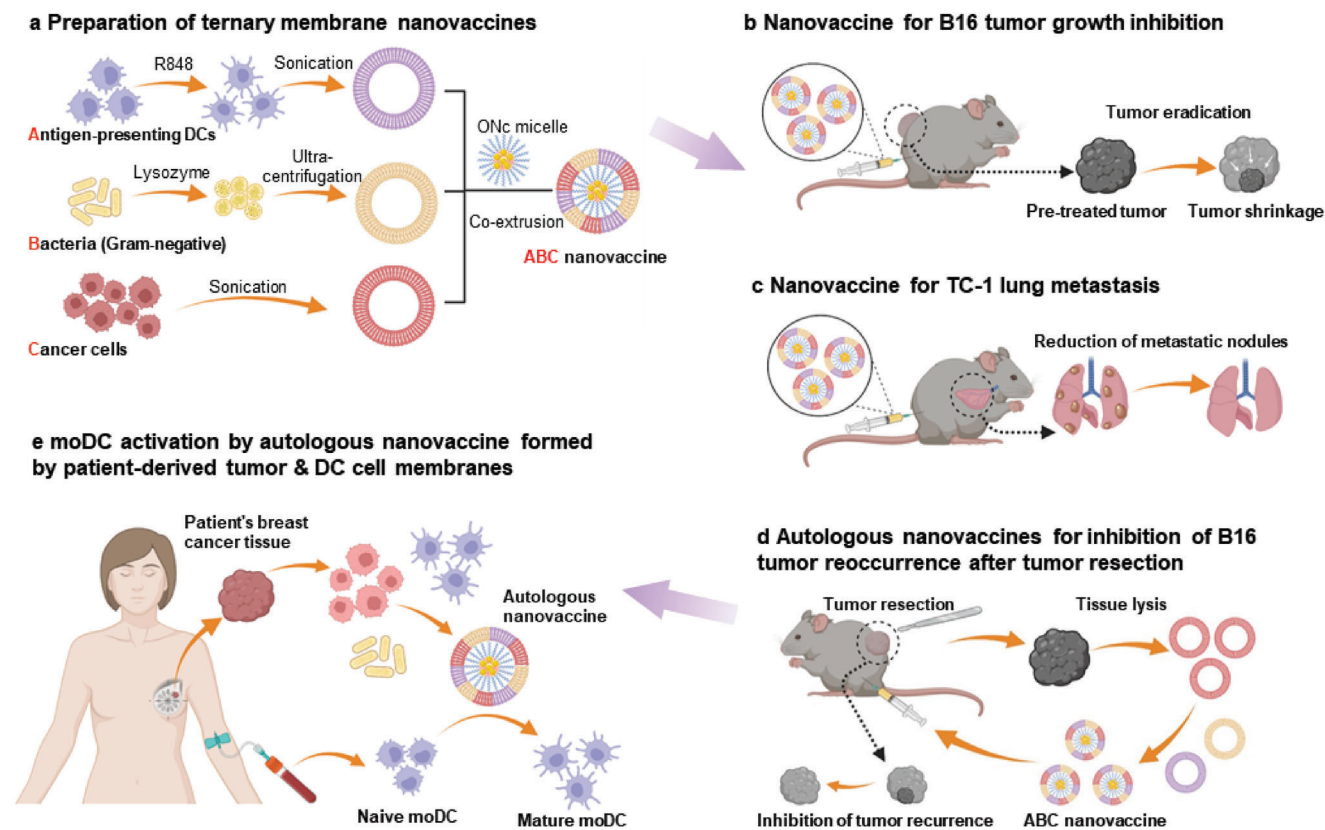


Figure 1. Schematic illustration of ABC nanovaccine preparation using ternary membrane systems including Antigen-presenting DC membrane, Bacterial membrane, and Cancer cell (either B16 or TC-1) membrane for different cancer immunotherapy applications.

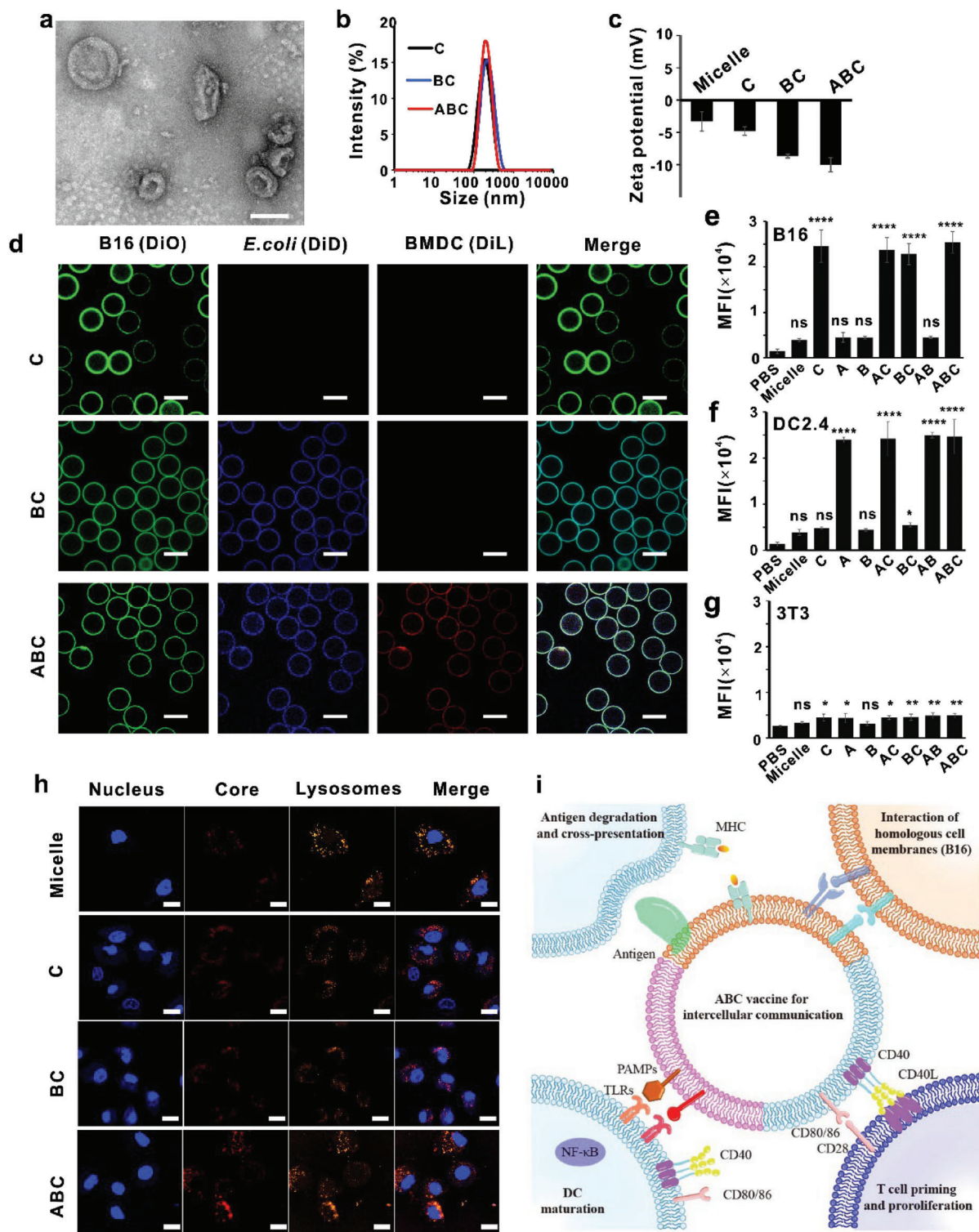
coating of C, BC, and ABC as shown in Figure 2c To analyze the chimeric status of different cell membrane components after co-extrusion, we labeled proteins on membranes of B16 cells and DCs by Cy3 and Cy5, respectively. As shown in Figure S10, Supporting Information, fluorescence resonance energy transfer (FRET) occurred for the coextrusion of B16 and DC membranes with higher Cy5 fluorescence than the group only containing each single membrane.

This suggests that proteins from two membranes were well-mixed on nanoparticles after coextrusion rather than forming nanoparticles comprising separate phases of membrane components. Furthermore, we used flow cytometry to validate the chimerism of different cell membrane components on individual nanoparticle. Before coextrusion, membrane of B16 cells, DCs and *E. coli* were labeled by DiO, DiL, and DiD fluorescent dyes, respectively. As shown in Figure S11, Supporting Information, over 70% nanoparticles of ABC group were composed of three membranes. Furthermore, to intuitively image the ternary membrane system under confocal microscope, we next employed SiO₂ microspheres with size of 10 μm instead of ONC-F127 nanoparticles as a supporting scaffold, taking advantage of the property of SiO₂ microspheres adsorbing phospholipid bilayers. C, BC and ABC membranes were coated onto microspheres by coincubation. It was shown again that the components of the hybrid membrane were evenly distributed but not in a phase separation state (Figure 2d). We also examined whether ABC is immunologically functional by conducting the flow cytometry analysis of ABC and

controls as indicated. As shown in Figure S12, Supporting Information, ABC ternary membrane system could effectively display co-stimulatory molecules such as CD40 and CD86 on the surface.

2.2. Cellular Engagement of the Ternary Membrane Vaccine

To examine whether the addition of cell membranes facilitates the interaction between nanovaccines and cancer or immune cells, micelles (ONC encapsulated F127 micelles without any membrane coating) and nanovaccines coated by single, binary and ternary membranes were incubated with B16 tumor cells as well as DC2.4 cells and 3T3 fibroblast cells as controls. DiL fluorescent dyes were loaded in micelles before coextrusion and cellular uptake of different formulations by cells were quantified by measurement of intracellular fluorescence intensity. All nanovaccines containing B16 cell-derived membranes showed good homologous cell membrane affinity for B16 tumor cells (Figure 2e). The fluorescence from B16 cells was 5.5 times higher than those from DCs and *E. coli*, respectively. The fluorescence from tri-membranes group ABC is 5.6 times higher than group DE. Similarly, cell membranes of mature DCs also facilitate intracellular uptake of vaccines in DC2.4 cells, since the fluorescence from tri-membranes group ABC is 4.5 times higher than group BC (Figure 2f). No significant difference was observed when nanovaccines were incubated with 3T3 cells (Figure 2g).



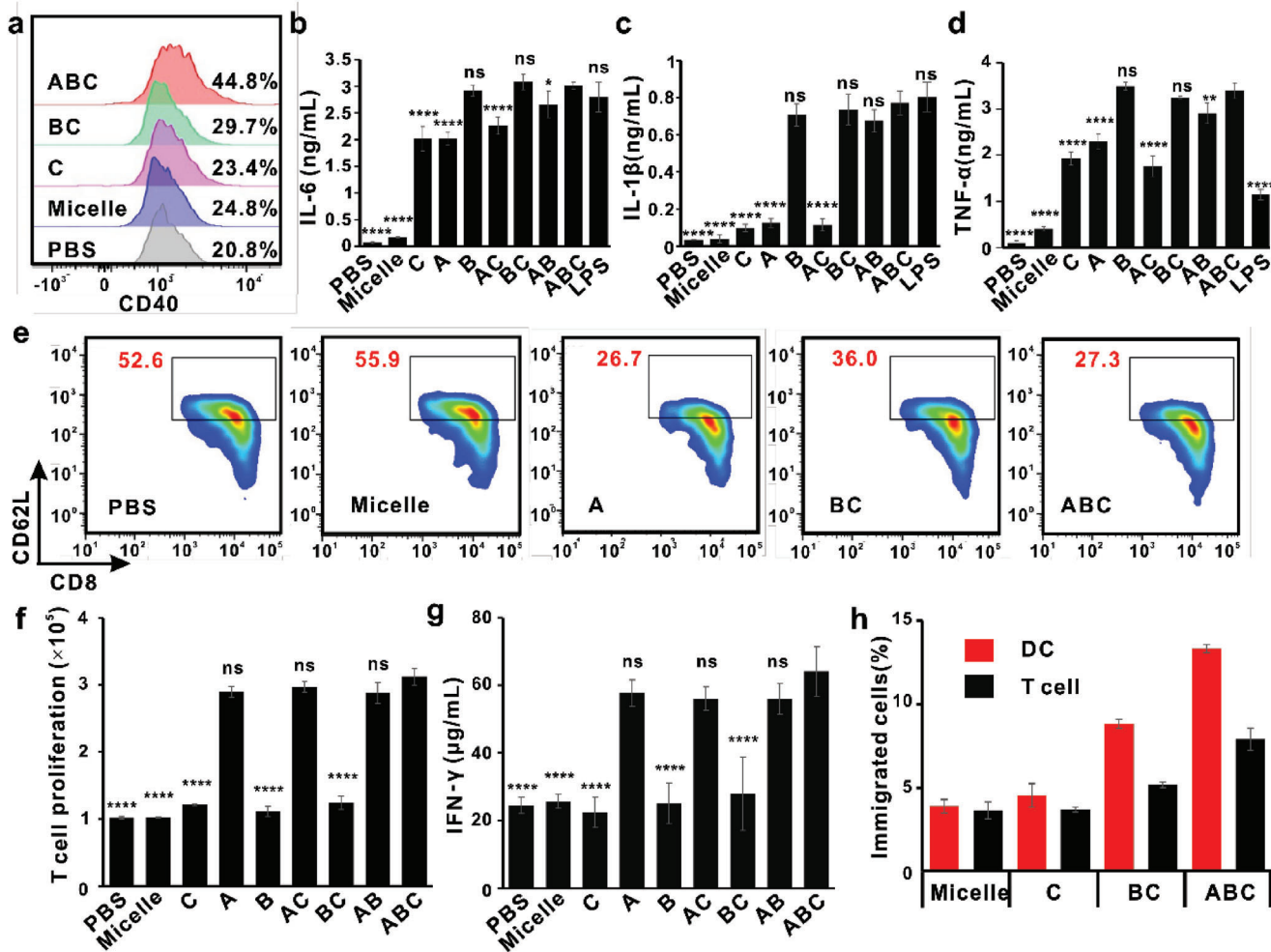


Figure 3. In vitro DC and T cell activation by of C, BC, and ABC. a) Expression of CD40 in CD11c⁺ BMDCs incubated with various formulations as indicated for 24 h. b–d) Proinflammatory cytokine concentrations of IL-6, IL-1 β , and TNF- α in DC supernatants after culture with various formulations as indicated after 24 h ($n = 3$; mean \pm SD). e) Expression of naive T cells (CD3⁺CD8⁺CD62L⁺) after treatment with various formulations as indicated for 48 h ($n = 3$; mean \pm SD). f) Quantification of the proportion of T cells co-cultured various formulations for 48 h ($n = 3$; mean \pm SD). g) Proinflammatory cytokine concentrations of IFN- γ in T cells supernatants after coculture with various formulations after 48 h ($n = 3$; mean \pm SD). h) Proportion of migrated cells after various formulations were incubated with DCs and T cells together, black: T cell; red: DC ($n = 3$; mean \pm SD). Significance was analyzed by one-way ANOVA with Bonferroni's post hoc test. All groups were compared with ABC. * $p < 0.05$, ** $p < 0.01$, *** $p < 0.001$, and **** $p < 0.0001$.

To further characterize the interaction of nanovaccines and immune cells, DC2.4 cells were used to incubate with vaccines C, BC, and ABC for 4 h. The micelles were labeled by DiI and lysosomes were stained by Lyso-tracker dye under confocal microscope. The addition of homologous cell membranes increased the uptake of DC2.4 cells compared with the micelle group. ABC group showed highest fluorescence signal, as shown in Figure 2h. These results demonstrate the superiority of tri-membrane-based ABC vaccine as a bridge to enhance the cell communications, which could first facilitate uptake by targeting DCs. Furthermore, antigen-presentation is an important step to activate DCs and T cells and this relies on the intercellular communication within a short distance. This hybrid membrane coated nanovaccine with simultaneously enhanced intercellular communications could facilitate the activation of immune cells and the following killing process of tumor cells. And the process was illustrated in Figure 2i.

2.3. In Vitro Immune Cell Activation

Membranes from bacteria usually contain pathogen-associated molecular patterns (PAMPs) that can induce the activation of specific immune cells. Besides, mature DC membrane loaded co-stimulatory molecules could interact with naive DCs and directly prime downstream immune cells. To investigate the properties of priming DCs, various formulations were cultured with naive bone marrow-derived dendritic cells (BMDCs) for 24 h, followed by the analysis of representative cytokines in medium and co-stimulation markers on BMDC membranes. Micelles and C group did not show remarkable increased expression of CD40 on BMDCs compared with PBS group (Figure 3a). The addition of bacterial membrane slightly increased the expression of CD40 (from 24.8% to 29.7%), likely because of PAMPs present in vaccines. After coating with membranes of mature DCs, ABC nanovaccine elicited stronger immune activation with 44.8% of

naive DCs expressing CD40 (Figure 3a). Mature BMDCs had higher secretion of proinflammatory cytokines (Figure 3b–d). We evaluated interleukin 6 (IL-6), tumor necrosis factor α (TNF- α), and interleukin 1 β (IL-1 β) and analyzed the effectiveness of each individual membrane component. The secretion level of IL-6 was substantially increased by the addition of cell membrane components, suggesting that cancer cell-derived antigens, dendritic cell-derived co-stimulatory molecules and bacterial membrane-derived PAMPs are effective in stimulating the production of this pro-inflammatory cytokine. In particular, BC and ABC vaccine had more IL-6 secretion as they both contain bacterial membrane compared to C vaccine only containing tumor cell membrane (Figure 3b). The addition of bacterial cell membranes appears to affect more on the expression of IL-1 β and TNF- α . The concentration of IL-1 β and TNF- α in medium of ABC group were 771 and 3394 pg mL⁻¹, respectively compared to BD group having 114 pg mL⁻¹ IL-1 β and 1759 pg mL⁻¹ TNF- α , respectively (Figure 3c,d). TLR-4 agonist LPS (1 μ g mL⁻¹) was used as a positive control for the study. These results indicate that ABC nanovaccines enhance the activation of DCs by upregulation of co-stimulator molecules and secretion of pro-inflammatory.

Next, we simulated the interaction between nanovaccines and T cells in lymph nodes in vitro. By flow cytometry sorting, we obtained cytotoxic T cells (CD8⁺CD3⁺) and incubated them with various formulations for T cell activation, followed by analyzing CD62 protein expression. As shown in Figure 3e, nanovaccines contain mature dendritic cells decreased naive T cells (CD62L⁺) to 26.7% compared with micelle group (55.9%). Meanwhile, ABC group containing three types of membranes decreased naive T cells (CD62L⁺) to 27.3%, suggesting the most effective T cell activation by ABC nanovaccines. In addition, the effect of nanovaccines in promoting T cell proliferation was also studied. After incubation with ABC vaccine for 48 h, quantities of T cells increased by 3.13 times, whereas the quantities of BC group increased by only 1.24 times (Figure 3f). This suggests that the addition of mature DC derived membranes could significantly induce the activation and proliferation of T cells. Medium supernatants from the incubation process were also collected for the determination of the important tumoricidal related cytokine interferon γ (IFN- γ). ABC nanovaccine incubated T cells secreted 2.29 times of IFN- γ compared to BC group (Figure 3g). Furthermore, we used trans-well assay to evaluate the impact of nanovaccines on the chemotaxis of DCs and T cells. B16 tumor cells were seeded at the bottom chamber and DCs and T cells were separately or together seeded in the upper chamber. After stimulation with ABC nanovaccine, cells migrating to the bottom chamber were counted using flow cytometry. Compared to the other formulations, both DC and T cell migration rates in the ABC group were significantly increased by 2.92- and 2.13-fold, respectively, compared to the C and BC group (Figure 3h). These results indicate that ABC nanovaccines could promote activation and proliferation of T cells, and increase the secretion of cytokines secretion which ultimately facilitates tumor immunotherapy.

2.4. DC Maturation and Specific T-Cell Responses In Vivo

Since ABC nanovaccine could enhance DC maturation and T cell activation, we hypothesize that the codelivery of ternary mem-

brane coated nanovaccines results in synergistic stimulation of an immune response, compared to single or binary membrane vaccines. As the lymph nodes are important organ for immunity, we investigated the accumulation of different nanovaccines in lymph nodes. After 24 h of subcutaneous injection, inguinal lymph nodes were harvested for IVIS imaging. It was demonstrated that the incorporation of DC cell membranes resulted in more accumulation of nanovaccines in lymph nodes. As shown in Figure S13, Supporting Information, the ABC vaccine with DC cell membrane had higher fluorescence in lymph node than that of the BC vaccine. To verify the hypothesis above, female C57BL/6 mice were subcutaneously inoculated with murine B16 tumor cells. Immunotherapy started by subcutaneous injection of nanovaccines three times every 7 days interval when the tumor volume reached ≈ 100 mm³. 3 days after the last injection, inguinal lymph nodes (LNs), spleens and tumors were collected for DC and T cell immune activation studies. As shown in Figure 4a,b, the expression of stimulatory markers (CD40 and/or CD80) on DCs in LNs was significantly enhanced after vaccination by BC and ABC nanovaccines. The percentage of CD40⁺CD86⁺ cells in CD11c⁺ cells were 21.45% (C), 28.97% (BC) and 42.96% (ABC), respectively. These results are consistent with the result of DC cell maturation in vitro. Since T cell proliferation and activation also occur in LNs, the percentage of CD8⁺CD3⁺cytotoxic T cells after vaccination was also investigated and found to be 22.1% (C), 27.67% (BC), and 31.47% (ABC), respectively (Figure 4c,d). We also studied T cell activation in the spleen, where the percentage of CD8⁺CD3⁺cytotoxic T cells after vaccination was 5.25% (C), 9.77% (BC) and 14.9% (ABC), respectively (Figure 4e,f). The immunotherapy effect in tumors was also investigated and the percentage of CD40⁺CD86⁺ cells in CD11c⁺ cells were 32.1% (C), 47.8% (BC), and 67.5% (ABC) in tumors, respectively (Figure 4g,h). Such significant increase indicates that ABC nanovaccine reprogrammed the immune suppression environment in tumors and stimulated the activation of the immune system and the recruitment of effector cells.

To analyze antigen specific T cells, splenocytes were collected after final vaccination by various vaccines. As shown in Figure 4i, IFN- γ ELISPOT kit was used to evaluate IFN- γ generation by the T cells from mice vaccinated by different nanovaccines. A few positive spots (average number: 1.7) were observed in the micelle and C group, whereas BC group had average 23 spots and the number of ABC group was 515, showing that the ternary system vaccine exhibited about 14 and 304 times more immune response than binary and single-membrane system vaccines (Figure 4j). Tetramer staining of specific cytotoxic T cells in spleen T cells of B16OVA tumor bearing mice illustrated that the ternary membrane system ABC vaccine increased the proportion of specific cytotoxic T cells corresponding to the OVA_{257–264} peptide from 2.56% to 7.96% (Figure S14, Supporting Information). Flow cytometry analysis of T cells in tumors showed that ABC nanovaccine effectively increased the proportion of T cells in tumors (from 14.8% to 26.7%) (Figure S15a, Supporting Information). Further analysis showed an increase in the proportion of CD8⁺ T cells in the T cell population (Figure S15b, Supporting Information) The ABC nanovaccine compared with antigen and adjuvant co-delivery group, has better immune activation effect, especially for specific immune activation, which is more conducive to the specific recognition and cytotoxic effect needed in tumor

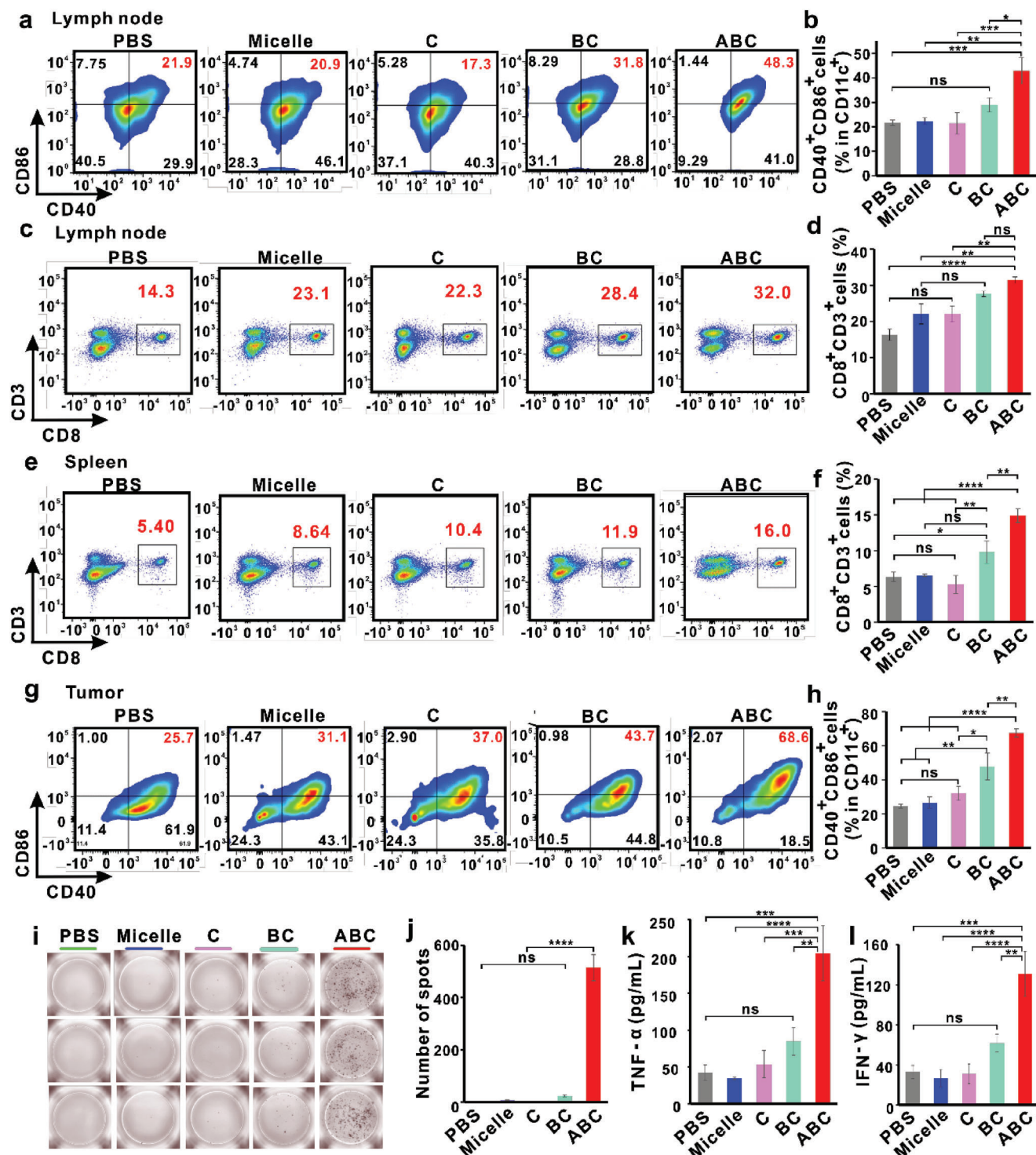


Figure 4. In vivo antitumor immune activation following immunization with C, BC, and ABC. a) Representative flow cytometric plots and b) quantification of mature DCs (CD11c⁺CD40⁺CD86⁺) in lymph nodes from mice at 3 days after vaccination by various formulations ($n = 3$; mean \pm SD). c) Representative flow cytometric plots and d) quantification of cytotoxic T cells (CD3⁺CD8⁺) in lymph nodes from mice on day 3 after vaccination ($n = 3$; mean \pm SD). e) Representative flow cytometric plots and f) quantification of cytotoxic T cells (CD3⁺CD8⁺) in spleens from mice on day 3 ($n = 3$; mean \pm SD). g) Representative flow cytometric plots and h) Quantification of mature DCs (CD11c⁺CD40⁺CD86⁺) in tumor from mice on day 3 after vaccination by various formulations ($n = 3$; mean \pm SD). i) Photos and j) corresponding quantification numbers of spots in the IFN- γ ELISPOT assay ($n = 3$; mean \pm SD). k, l) Proinflammatory cytokine concentrations of IFN- γ and TNF- α in serum from mice on day 3 after vaccination by various formulations ($n = 3$; mean \pm SD). Significance was analyzed by one-way ANOVA with Bonferroni's post hoc test. * $p < 0.05$, ** $p < 0.01$, *** $p < 0.001$, and **** $p < 0.0001$.

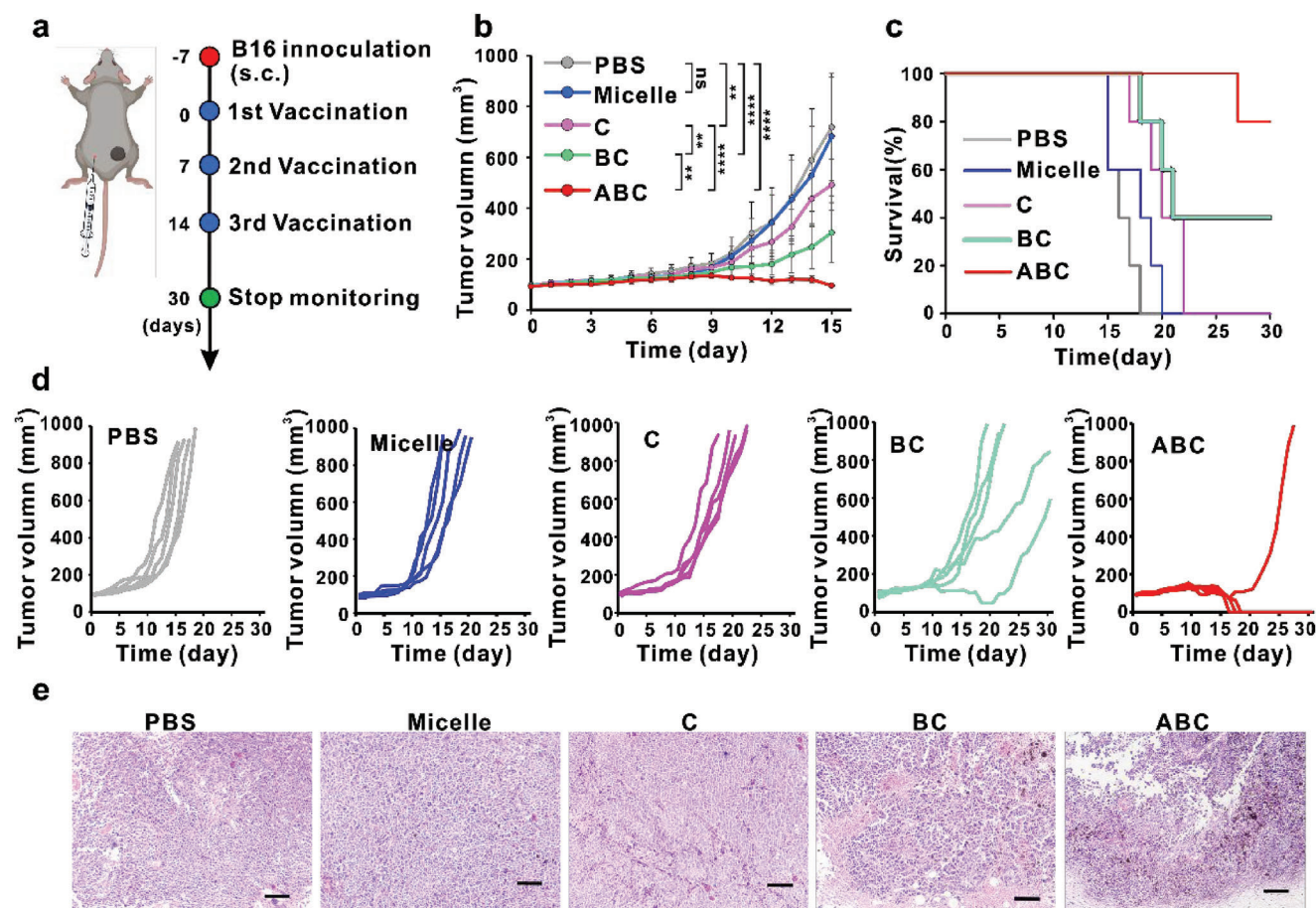


Figure 5. Tumor growth suppression by immunization with C, BC, or ABC. a) Scheme of immunotherapy treatment by various formulations. Subcutaneous injections of 100 μ L different formulations containing 12 μ g of B16 membrane protein, 10 μ g of *E. coli* membrane protein and 11 μ g of mature DCs membrane protein were given per mouse for each immunization. b) Average tumor volume after B16 tumor-bearing mice were treated by different vaccines as indicated ($n = 5$; mean \pm SD). c) Survival curve of different groups treated by different vaccines. d) Individual B16 tumor growth curve after mice were given PBS, Micelle, C, BC, or ABC vaccines. e) H&E staining of tumors tissue sections from mice after various treatments. Significance was analyzed by two-way ANOVA with Tukey post-hoc test. * $p < 0.05$, ** $p < 0.01$, *** $p < 0.001$, and **** $p < 0.0001$.

immunotherapy. The increased level of cytotoxic T cells was also accompanied with the increase of cytokines. ABC nanovaccine exhibited enhanced level of TNF- α and IFN- γ in plasma, significantly higher than other control groups (Figure 4k,l).

2.5. Tumor Immunotherapy with the ABC Vaccine

To investigate the antitumor efficacy of ABC nanovaccine, C57BL/6 mice were injected subcutaneously with 1×10^6 B16 cells per mouse. Then tumor-bearing mice were subcutaneously injected by various formulations including PBS, micelles, C, BC and ABC nanovaccines for three times every 7 days (Figure 5a for treatment scheme). Tumor volume and body weight were monitored every day. As the tumor volume reached 1000 mm^3 , mice were sacrificed and the volume of tumors were shown in Figure 5b. Tumor growth of mice treated with C nanovaccines was slightly delayed compared with the PBS and micelle group. For the BC nanovaccine group, tumor growth was significantly delayed. In contrast, ABC nanovaccine showed no significant

increase of tumor volume growth, indicative of the excellent anti-tumor efficacy by ABC vaccination. No overt acute toxicity was observed since no significant body weight change occurred in any group (Figure S16, Supporting Information). The ABC group demonstrated the best therapeutic efficacy with 4 of 5 mice cured (Figure 5c). The growth of individual tumor in each group is also illustrated in Figure 5d. On day 30, all tumors were collected and the representative H&E staining images were showed in Figure 5e. Sections of other major tissues were shown in Figure S17, Supporting Information. All formulations had no significant tissue toxicity compared to PBS group. In tumor tissue of mice vaccinated by ABC vaccine showed significant apoptosis and increased tissue voids.

2.6. Generalization of ABC for Additional Anti-Cancer Applications

To generalize the ternary membrane nanovaccine system, we further tested the therapeutic efficacy of the ABC vaccine in

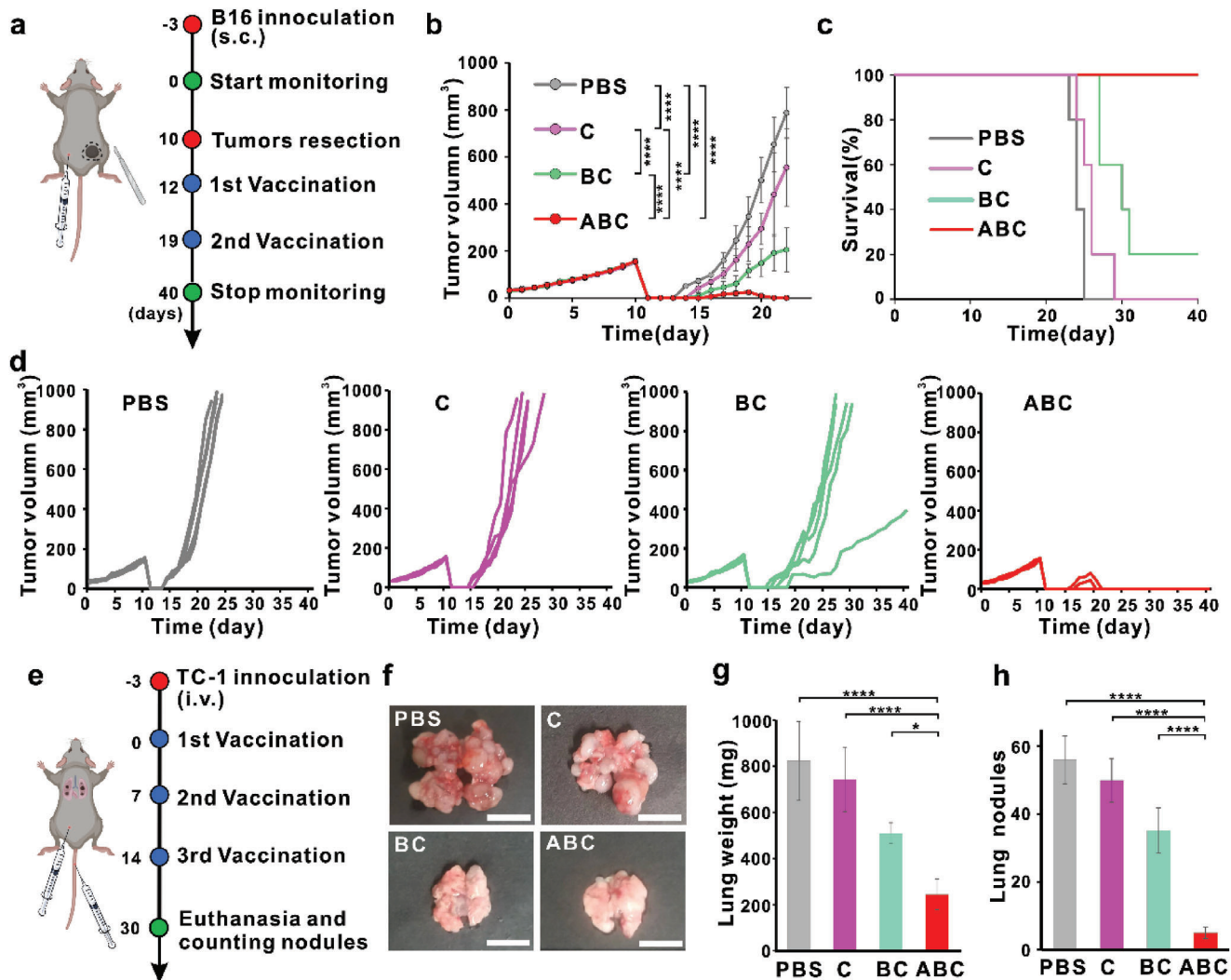


Figure 6. Generalization of ternary membrane nanovaccines for prevention of postoperative tumor recurrence after vaccination of autologous vaccine, lung metastasis prevention using membrane of another cancer type. a) Scheme of immunotherapy treatment by various formulations after surgical removal of tumor, followed by vaccination by autologous vaccines. Subcutaneous injections of 100 μ L formulation containing 12 μ g of B16 membrane protein, 10 μ g of *E. coli* membrane protein and 11 μ g of mature DCs membrane protein were given per mouse for each immunization. B16 membrane were obtained by cell extraction from autologous excised tumor tissue. b) Average tumor volume during surgery and treatment by different vaccines as indicated ($n = 5$; mean \pm SD). c) Survival curve of different groups treated by different vaccines as indicated. d) Individual B16 tumor growth curve after mice were given PBS, B, BC, or ABC vaccines. e) Scheme of immunotherapy treatment for the prevention of lung metastasis model by various formulations using TC-1 cells. Subcutaneous injections of 100 μ L formulation containing 12 μ g of TC-1 membrane protein, 10 μ g of *E. coli* membrane protein and 11 μ g of mature DCs membrane protein were given per mouse for each immunization. f) Representative lung tissue photographs of each group. Scale bar: 1 cm. g) Weight of lung tissue in each group ($n = 5$; mean \pm SD). h) Statistical results of the number of metastatic nodules in lung tissue in each group ($n = 5$; mean \pm SD). Figure 2b was analyzed by two-way ANOVA with Tukey post-hoc test and others were analyzed by one-way ANOVA with Bonferroni's post hoc test. * $p < 0.05$, ** $p < 0.01$, *** $p < 0.001$, and **** $p < 0.0001$.

multiple more clinically relevant scenarios including treatment with surgical removal of tumor and formation of autologous tumor membrane-based vaccines, evaluation of another tumor cell membrane in a lung metastasis model and vaccine preparation from human-derived cancer cells. Surgical excision of tumor lesions is a common treatment method, but incomplete excision of tumor tissue often leads to tumor recurrence and metastasis within a short period of time. Tumor cell membranes obtained from resection were used to prepare the corresponding ternary membrane nanovaccine, which effectively in-

hibited tumor recurrence and avoided the hassle of identification and screen of tumor-specific antigens. In the surgical resection model, C57BL/6 mice were injected subcutaneously with 1×10^6 B16 cells per mouse and tumors were surgically removed when the tumor volume reached ≈ 150 mm³ (on day 10). The nanovaccine, prepared by cancer cell membranes from each individual mouse tumor, was injected back to the same mouse on day 12 and day 19. Tumor volume and body weight were monitored every day (Figure 6a). As the tumor volume reached 1000 mm³, mice were sacrificed and the volume of tumors were shown in

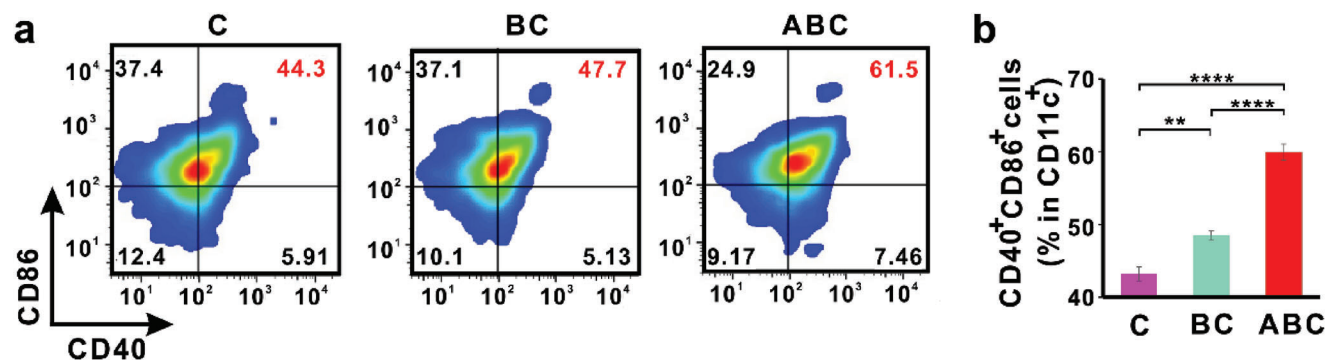


Figure 7. ABC nanovaccines prepared by human-derived tumor cells for the activation of the patients' own MoDCs. a) Representative flow cytometric plots and b) quantification of mature DCs (CD11c⁺CD40⁺CD86⁺) of human-derived DC cells ($n = 3$; mean \pm SD). Significance was analyzed by one-way ANOVA with Bonferroni's post hoc test, * $p < 0.05$, ** $p < 0.01$, *** $p < 0.001$, and **** $p < 0.0001$.

Figure 6b. Tumor growth of mice treated with C nanovaccines was slightly delayed compared with the PBS group. For the BC nanovaccine group, tumor growth was significantly delayed. In contrast, the ABC nanovaccine demonstrated no tumor recurrence in three of the five mice after the first treatment. For the rest two, after the second treatment, no recurrence was also observed within 40 days. The ABC group showed the best treatment effect, with all mice surviving until day 40 and no tumor recurrence was observed (Figure 6c,d). In addition, no significant body weight change was observed in any group, suggesting no overt acute toxicity of ABC vaccine (Figure S18, Supporting Information). To study the therapeutic effect of nanovaccines on cancer metastasis, we used another cancer cell type (cervical cancer TC-1 cell instead of B16 cancer cell) for the preparation of the ternary membrane vaccine. C57BL/6 mice were intravenously injected with 5×10^5 TC-1 cells per mouse and subcutaneously injected by various formulations including PBS, C, BC, and ABC nanovaccines for three times with 7 days interval (Figure 6e). After 30 days, the mice were euthanized and their lung tissue were collected. Metastases in the lungs of mice were observed in the PBS and C groups, whereas less metastasis were seen in the BC and ABC group. The number of metastatic nodules in lungs (Figure 6f) and lung weight (Figure 6g) were also recorded, showing that the ABC vaccine substantially reduced the metastasis of TC-1 cancer cells compared to the other control groups (Figure 6g,h). One of limitations of this experiment was that the duration between rechallenge was too short to establish meaningful tumor memory responses, but these results illustrate the effectiveness of ternary membrane-based nanovaccines for prevention of post-surgical cancer recurrence and metastasis.

To further investigate the clinical translation potential of this ternary membrane nanovaccine, ABC vaccine was formed using human-derived DC and cancer cells collected from three patients, followed by evaluation of the activation of the patients own moDC. It was shown that binary membrane nanovaccines (BC) have better DC cell activation than cancer cell membrane nanovaccines (C) alone, while ternary nanovaccines (ABC) containing human-derived mature DC cell membranes have the highest immune activation effect (Figure 7a). As shown in Figure 7b, ABC nanovaccine stimulated DC cells (CD11c⁺) population expressed both co-stimulatory factors CD40 and CD86 ac-

counting for over 60%, showing the potential of ABC's clinical applications.

3. Conclusion

In summary, a nanovaccine coated with ternary membranes including tumor cell membranes, bacterial membranes and dendritic cell membranes was generated and each membrane component conferred distinct functions for anti-tumor immunity. Cancer cell derived membranes provided a broad base of tumor antigens to prevent immune evasion against a single target, while bacteria cytoplasmic membranes with PAMPs acted as adjuvants and avoided side effects such as cytokine storm from cell wall fractions. The addition of membranes from DCs achieved multiple cellular interactions and enhanced adaptive immune response against specific tumor targets. In tumor-bearing murine models, ABC vaccine has good antitumor efficacy with prolonged survival time. The ternary membrane system also showed potent therapeutic effect without cancer recurrence in a more clinically-relevant surgical resection model. The methodology can also be generalized using membranes of another murine tumor cell type and also actual human cancer cells. Overall, the ternary membrane system nanovaccine approach demonstrated a new multicellular communication platform with potential to be used for effective anticancer immunotherapy. Future directions of research may include in-depth mechanistic investigation on effector CD8⁺ T cells, memory T cells and immune suppressive cells and further evaluation of clinical translation potential using models of patient-derived tumor tissues.

4. Experimental Section

Materials and Reagents: Pluronic F127 and ONc (5,9,14,18,23,27,32,36-octabutoxy-2,3-naphthalocyanine) were purchased from Sigma-Aldrich. SiO₂ microspheres (diameter 10 μ m) were purchase from YUAN BIOTECH. The fluorescent dye of DiD, DiO, and DiL were purchased from US Everbright Co. The fluorescent dyes Cy3 and Cy5 were purchased from Yuanye Bio-Technology Co. Antibodies against mouse CD11c-APC (catalogue no. 117 309), anti-CD40-FITC (catalogue no. 102 905), anti-CD86-Percp-Cy5.5 (catalogue no. 105 027), anti-CD8a-APC (catalogue no. 100 712), anti-CD3-FITC (catalogue

no. 100 203) and against human CD11c-APC (catalogue no. 301 613), anti-CD40-FITC (catalogue no. 334 305), anti-CD8 6-Percp-Cy5.5 (catalogue no. 374 215) were purchased from Biologend. MHC I-strep for SIINFEKL (catalogue no. 6-7015-001) and PE-Strep-Tactin (catalogue no. 6-5000-001) were purchased from IBA Life science. Recombinant mouse GM-CSF, human GM-CSF, and human IL-4 were obtained from Genscript. TNF- α mouse ELISA kit (catalogue no. SEKM-0034), IFN- γ mouse ELISA kit (catalogue no. SEKM-0031), DAPI and peripheral blood mononuclear cell extraction kit were purchased from Solarbio. Lyso-tracker Red (catalogue no. C1046) were obtained from Beyotime Biotechnology. B16 cells and B16OVA cells were kindly provided from professor Shaokai Sun and DC2.4 cells were purchased from Bena culture collection. *E. coli* Nissle 1917 was purchased from Biobw Bio-Technology Co.

Preparation of F127 Micelles: 0.1 mg ONc was dissolved in 0.1 mL dichloromethane chloride and added to 1 mL 10% (wt) F127 aqueous solution. The mixture was stirred for 3 h and then subjected to ultrafiltration at 4 °C twice to remove excessive F127 to make ONc encapsulated F127 micelles with good stability. Finally, the final volume was fixed to 1 mL.

Extraction of Cell Membrane: BMDCs were prepared as described previously.^[35] Briefly, monocytes were collected in bone marrow of 6–8 weeks C57BL/6 mice and cultured in Roswell Park Memorial Institute (RPMI) 1640 medium containing GM-CSF with 5% CO₂ at 37 °C for 6 days. Then BMDCs were treated with 40 ng mL⁻¹ R848 for maturation for 48 h. BMDCs were collected, resuspended in PBS and sonicated for 5 min (2 s on/off, power of 60 W). The mixture was centrifugated at 1000×g for 10 min at 4 °C to obtain cell membranes in the supernatant. For B16 tumor cells, collected cells were resuspended in PBS and sonicated for 5 min (2 s on and 2 s off, power at 60 W). The mixture was subjected to centrifugation at 1000×g for 10 min at 4 °C to obtain cell membranes in the supernatant.

Extraction of Cytoplasmic Membranes from *E. coli*: Briefly, freeze-preserved *E. coli* 1917 were cultured in LB medium at 37 °C overnight. Upon reaching an OD₆₀₀ of 1.2, the bacteria were collected by centrifugation (3000×g, 20 min, 4 °C) and washed three times with PBS. 10 mL buffer A (1 M sucrose, 0.2 M Tris-HCl, pH 8.0) with lysozyme at 2 mg mL⁻¹ was added to cell pellet. The cells were incubated at 37 °C with shaking at 120 rpm for 1 h. Sterile water (90 mL) supplemented with DNase (10 μ g mL⁻¹) was added and the tube was gently mixed 20 times. Spheroplasts were collected by centrifugation at 3000×g for 20 min at 4 °C and resuspended in 10 mL ice-cold buffer B (20 mM Tris-HCl, pH 7.2, 50 mM NaCl, 5 mM EDTA) containing 20% w/v sucrose to lyse the cells. The lysate was purified to remove cell debris by centrifugation at 10 000×g for 30 min at 4 °C. The membranes were collected by centrifugation at 113 000×g for 1 h at 4 °C, and then resuspended in PBS for the following experiments.

Preparation of ABC Nanovaccines: Protein concentration of membranes were quantified by using BCA protein assay kit and the protein concentration of the membrane solution was diluted to 1 mg mL⁻¹ (B16 membrane solutions), 0.33 mg mL⁻¹ (*E. coli* membrane solutions) and 0.6 mg mL⁻¹ (mature BMDC membrane solutions), respectively. 50 μ L of 10% (wt) ONc F127 micelles, 60 μ L B16 membrane solutions, 150 μ L *E. coli* membrane solutions, 90 μ L mature BMDC membrane solutions and 150 μ L PBS were mixed and extruded by extruder (LP-1, Jungao)

equipped with 200 and 100 nm membrane cut-off for 7 circles for each. C and BC nanovaccines were prepared similarly without addition of membrane components of AB or A.

Characterization of Nanovaccines: Size and Zeta potential were measured by Zetasizer (Nano ZS, Malvern). Morphology of micelles were observed using transmission electron microscopy (JEM-F200, JEOL). For co-location studies, membranes of B16, *E. coli* and mature BMDC were labeled by DiO, DiD and DiL and then analyzed by flow cytometry (FACS Verse, BD).

Preparation of SiO₂ Microsphere-Supported ABC Ternary Membrane: SiO₂ microsphere-supported bilayers were synthesized as described before.^[36] Briefly, SiO₂ microspheres (with diameter of 10 μ m) were suspended in a 1 mL solution of 4% H₂O₂ and 4% NH₄OH and immersed in a water bath at 80 °C for 10 min. After being rinsed with distilled water, the SiO₂ microspheres were resuspended in a 1 mL of 4% H₂O₂ and 0.4 M HCl solution and placed in a water bath at 80 °C for 10 min. The SiO₂ microspheres were then rinsed with deionized water several times. After final centrifugation, the SiO₂ microspheres were resuspended in PBS for further use. Membranes of B16, *E. coli* and mature BMDC were labeled by DiO, DiD, and DiL, respectively. SiO₂ microspheres were added to the mixture solution of B16 membrane, *E. coli* membrane and mature BMDC membrane, then subjected to shaking for 45 min. Free membranes were removed by centrifugation at 2000×g for 2 min, and washing twice with PBS. SiO₂ microsphere-supported C and BC membrane were prepared using the similar protocol without addition of AB or A components. Afterward, SiO₂ microspheres were observed under confocal laser scanning microscope (A1R+, Nikon).

Cellular Uptake and Intracellular Distribution: For cellular uptake study, B16 cells, DC2.4 cells and 3T3 cells were plated in 6-well plates with 1 \times 10⁶ cells per well and incubated with 50 μ L of various formulations including micelle, C, BC and ABC nanovaccines for 4 h at 37 °C with 5% CO₂. Afterward, cells were collected and lysed by 1% Triton X-100. Mean fluorescence intensity was measured with microplate reader. For the intracellular distribution study, 1 \times 10⁶ DC2.4 cells incubated with 50 μ L of various formulations including micelle, C, BC, and ABC nanovaccines. After 4 h, cells were washed twice by PBS and incubated with Lyso-tracker Red and DAPI in PBS to stain lysosomes and nuclei. Then, BMDCs were observed under confocal laser scanning microscope (A1R+, Nikon).

In Vitro DC Activation: BMDCs were plated in 6-well plates with 1 \times 10⁶ cells per well. After 24 h, 50 μ L of various formulations were added in 1 \times 10⁶ naive BMDCs in complete media and then incubated for 24 h at 37 °C with 5% CO₂. BMDCs were harvested, washed twice with PBS and incubated with fluorophore-labeled antibodies against CD11c, CD40, and CD86 for 40 min. Cells were then washed twice by PBS, resuspended and analyzed by flow cytometry (FACS Aria III, BD). The supernatant of the culture medium was collected and used for evaluation of IL-6, IL-1 β , and TNF- α by the ELISA kits.

In Vitro T Cells Activation: CD8⁺ T cells were isolated from mouse spleen and sorted by flow cytometry (CD3⁺CD8⁺). CD8⁺ T cells were plated in 24-well plates with 1 \times 10⁵ cells per well and cultured with 10 μ L of various formulations for 48 h. Cells were harvested, washed twice with PBS and incubated with fluorophore-labeled antibodies against CD8, CD3 and CD62L for 40 min. Cells were then washed twice by PBS, resuspended

and analyzed by flow cytometry. The supernatant of the culture medium was collected and used for the ELISA kit of IFN- γ .

In Vivo Activation of DCs and T Cells: All animal experiments were performed in accordance with the guidelines and approved by the Animal Ethics Committee at the Tianjin University (no. TJUE-2021-025). Female C57BL/6 mice of age 6–8 weeks were immunized with different formulations in 100 μ L volume by subcutaneous injection at the tail base at indicated time points. 3 days after vaccination, the LNs spleens and tumors were collected and prepared to obtain single cell suspensions. Cells were stained with fluorophore-labeled antibodies against CD11c, CD40, and CD86 for DC analysis or fluorophore-labeled antibodies against CD8 CD3 for T cell analysis. The cytokines in serum including TNF- α and IFN- γ were analyzed by ELISA kits. For antigen specific ELISPOT analysis, splenocytes were collected and plated in ELISPOT plate with 1×10^5 cells per well and 10 μ L of B16 cell membrane formulations were added.

In Vivo Activation of Specific Cytotoxic CD8+ Cell: For the B16OVA tumor immunotherapy model, female C57BL/6 mice of age 6–8 weeks were subcutaneously injection 1×10^6 B16 cells. When the tumor volume reaches $\approx 100 \text{ mm}^3$, the mice were randomly divided into 5 groups (3 mice per group). Mice were vaccinated on day 0 and 7 by subcutaneous injection of various formulations. 7 days after vaccination, the splenocytes were isolated and stained with PE-labeled SIINFEKL-MHC I tetramer. CD8+ T cells were gated by anti-CD8 α -APC and anti-CD3-FITC and percentage of OVA_{257–264} specific CD8+ T cells were measured by flow cytometry.

In Vivo Vaccination and Cancer Immunotherapy Studies: For the B16 tumor immunotherapy model, female C57BL/6 mice of age 6–8 weeks were subcutaneously injected with 1×10^6 B16 cells. Body weight and tumor volume was measured every day. Tumor volume was calculated as width² \times length \times 0.5. When the tumor volume reaches $\approx 100 \text{ mm}^3$, the mice were randomly divided into 5 groups (5 mice per group). Mice were vaccinated on day 0, 7, and 14 by subcutaneous injection of various formulations. Mice were sacrificed when the tumor size reached 1000 mm^3 . For the B16 tumor surgical treatment model, female C57BL/6 mice of age 6–8 weeks were subcutaneously injection 1×10^6 B16 cells. Body weight and tumor volume was measured every day. Tumor volume was calculated as width² \times length \times 0.5. When the tumor volume reaches $\approx 150 \text{ mm}^3$, the mice were randomly divided into 4 groups (5 mice per group) and tumors were surgically removed on day 10. Mice were vaccinated on day 12 and 19 by subcutaneous injection of nanovaccines prepared from autologous tumor cells. Mice were sacrificed when the tumor size reached 1000 mm^3 . For the TC-1 tumor lung metastasis model, female C57BL/6 mice of age 6–8 weeks were intravenously injected with 5×10^5 TC-1 cells. Mice were vaccinated on day 0, 7, and 14 by subcutaneous injection of various formulations. Mice were sacrificed and lungs were collected on day 30. Lung weight was recorded and the number of metastatic nodules was counted.

In Vitro Human-Derived DC Activation: Human blood and tumor sample collection was in accordance with the Tianjin Medical University Institutional Review Board (no. TJMUE-2022-007). For the study of the therapeutic effect of human-derived ternary membrane nanovaccines, surgically removed tumor tissue and blood samples were collected from the same patient for three volunteers. Human-derived monocytes were subsequently isolated

using a peripheral blood mononuclear cell extraction kit and induced in medium containing recombinant human GM-CSF and IL-4 cytokines to obtain human-derived immature DC cells. 50 μ L of various formulations were added in 1×10^6 immature BMDCs in complete media and then incubated for 24 h at 37 $^\circ\text{C}$ with 5% CO₂. Then cells were harvested, washed twice with PBS and incubated with fluorophore-labeled antibodies against CD11c, CD40, and CD86 for 40 min. Cells were then washed twice by PBS, resuspended and analyzed by flow cytometry (FACS Aria III, BD).

Supporting Information

Supporting Information is available from the Wiley Online Library or from the author.

Acknowledgements

The authors thank Professor Shaokai Sun for kindly provided B16 cells. This work was supported by the National Key Research and Development Program (2021YFC2102300), the National Natural Science Foundation of China (32071384), the Start-up Grant at Tianjin University, the One-thousand Young Talent Program of China, and the National Institutes of Health (R01CA247771).

Conflict of Interest

The authors declare no conflict of interest.

Author Contributions

Y.Z. supervised the project. H.R. carried out most experiments. H.R. and Y.Z. conceived the project. J.L., J.Z., and Q.Q. assisted with animal experiments. J.L. and N.Z. assisted with material synthesis and characterization. D.L., Y.Y., and X.L. assisted with collection of human blood and tumor tissues from patients. H.R. and Y.Z. performed data analysis and wrote the manuscript, J.F.L. assisted with manuscript editing and provided valuable suggestions.

Data Availability Statement

The data that support the findings of this study are available in the supplementary material of this article.

Keywords

biomimetic materials, cancer immunotherapy, hybrid membrane, nanovaccine

Received: May 13, 2023

Revised: July 25, 2023

Published online:

[1] D. J. Irvine, E. L. Dane, *Nat. Rev. Immunol.* **2020**, *20*, 321.

[2] X. He, S. Zhou, W.-C. Huang, A. Seffouh, M. T. Mabrouk, M. T. Morgan, J. Ortega, S. I. Abrams, J. F. Lovell, *ACS Nano* **2021**, *15*, 4357.

- [3] R. Kuai, L. J. Ochyl, K. S. Bahjat, A. Schwendeman, J. J. Moon, *Nat. Mater.* **2017**, *16*, 489.
- [4] H. Liu, K. D. Moynihan, Y. Zheng, G. L. Szeto, A. V. Li, B. Huang, D. S. Van Egeren, C. Park, D. J. Irvine, *Nature* **2014**, *507*, 519.
- [5] D. S. Wilson, M. Damo, S. Hirose, M. M. Raczky, K. Brünggel, G. Diaceri, X. Quaglia-Thermes, J. A. Hubbell, *Nat. Biomed. Eng.* **2019**, *3*, 817.
- [6] H. Ren, J. Li, G. Liu, Y. Sun, X. Yang, Z. Jiang, J. Zhang, J. F. Lovell, *ACS Appl. Mater. Interfaces* **2022**, *14*, 2510.
- [7] I. Dagogo-Jack, A. T. Shaw, *Nat. Rev. Clin. Oncol.* **2018**, *15*, 81.
- [8] S. A. Rosenberg, J. C. Yang, N. P. Restifo, *Nat. Med.* **2004**, *10*, 909.
- [9] S. H. van der Burg, R. Arens, F. Ossendorp, T. van Hall, C. J. Melief, *Nat. Rev. Cancer* **2016**, *16*, 219.
- [10] X. Wei, M. Ying, D. Dehaini, Y. Su, A. V. Kroll, J. Zhou, W. Gao, R. H. Fang, S. Chien, L. Zhang, *ACS Nano* **2018**, *12*, 109.
- [11] D. Wang, S. Wang, Z. Zhou, D. Bai, Q. Zhang, X. Ai, W. Gao, L. Zhang, *Adv. Healthcare Mater.* **2022**, *11*, e2101349.
- [12] Y. Jiang, N. Krishnan, J. Zhou, S. Chekuri, X. Wei, A. V. Kroll, C. L. Yu, Y. Duan, W. Gao, R. H. Fang, L. Zhang, *Adv. Mater.* **2020**, *32*, 2001808.
- [13] R. H. Fang, C. M. Hu, B. T. Luk, W. Gao, J. A. Copp, Y. Tai, D. E. O'Connor, L. Zhang, *Nano Lett.* **2014**, *14*, 2181.
- [14] Z. Chen, Z. Wang, Z. Gu, *Acc. Chem. Res.* **2019**, *52*, 1255.
- [15] J. Xu, J. Lv, Q. Zhuang, Z. Yang, Z. Cao, L. Xu, P. Pei, C. Wang, H. Wu, Z. Dong, Y. Chao, C. Wang, K. Yang, R. Peng, Y. Cheng, Z. Liu, *Nat. Nanotechnol.* **2020**, *15*, 1043.
- [16] A. V. Kroll, R. H. Fang, Y. Jiang, J. Zhou, X. Wei, C. L. Yu, J. Gao, B. T. Luk, D. Dehaini, W. Gao, L. Zhang, *Adv. Mater.* **2017**, *29*, 03969.
- [17] T. Kang, Y. Huang, Q. Zhu, H. Cheng, Y. Pei, J. Feng, M. Xu, G. Jiang, Q. Song, T. Jiang, H. Chen, X. Gao, J. Chen, *Biomaterials* **2018**, *164*, 80.
- [18] F. Fontana, M. A. Shahbazi, D. F. Liu, H. B. Zhang, E. Makila, J. Salonen, J. T. Hirvonen, H. A. Santos, *Adv. Mater.* **2017**, *29*, 03239.
- [19] K. A. Fitzgerald, J. C. Kagan, *Cell* **2020**, *180*, 1044.
- [20] H. Petousis-Harris, J. Paynter, J. Morgan, P. Saxton, B. McArdle, F. Goodyear-Smith, S. Black, *Lancet* **2017**, *390*, 1603.
- [21] A. I. Camacho, J. M. Irache, J. de Souza, S. Sánchez-Gómez, C. Gamazo, *Vaccine* **2013**, *31*, 3288.
- [22] O. Y. Kim, H. T. Park, N. T. H. Dinh, S. J. Choi, J. Lee, J. H. Kim, S. W. Lee, Y. S. Cho, *Nat. Commun.* **2017**, *8*, 626.
- [23] J. Zhou, E. Karshalev, R. Mundaca-Urbe, B. Esteban-Fernandez de Avila, N. Krishnan, C. Xiao, C. J. Ventura, H. Gong, Q. Zhang, W. Gao, R. H. Fang, J. Wang, L. Zhang, *Adv. Mater.* **2021**, *33*, 2103505.
- [24] L. Chen, H. Qin, R. Zhao, X. Zhao, L. Lin, Y. Chen, Y. Lin, Y. Li, Y. Qin, Y. Li, S. Liu, K. Cheng, H. Chen, J. Shi, G. J. Anderson, Y. Wu, Y. Zhao, G. Nie, *Sci. Transl. Med.* **2021**, *13*, eabc2816.
- [25] C. Xu, Y. Jiang, Y. Han, K. Pu, R. Zhang, *Adv. Mater.* **2021**, *33*, 2008061.
- [26] G. Deng, Z. Sun, S. Li, X. Peng, W. Li, L. Zhou, Y. Ma, P. Gong, L. Cai, *ACS Nano* **2018**, *12*, 12096.
- [27] Y. Jiang, N. Krishnan, J. Zhou, S. Chekuri, X. Wei, A. V. Kroll, C. L. Yu, Y. Duan, W. Gao, R. H. Fang, L. Zhang, *Adv. Mater.* **2020**, *32*, 2001808.
- [28] M. H. Andersen, *Semin. Immunopathol.* **2022**, *45*, 253.
- [29] P. G. Coulie, B. J. Van den Eynde, P. van der Bruggen, T. Boon, *Nat. Rev. Cancer* **2014**, *14*, 135.
- [30] S. Kreiter, M. Vormehr, N. van de Roemer, M. Diken, M. Löwer, J. Diekmann, S. Boegel, B. Schrörs, F. Vascotto, J. C. Castle, A. D. Tadmor, S. P. Schoenberger, C. Huber, Ö. Türeci, U. Sahin, *Nature* **2015**, *520*, 692.
- [31] B. Ou, Y. Yang, W. L. Tham, L. Chen, J. Guo, G. Zhu, *Appl. Microbiol. Biotechnol.* **2016**, *100*, 8693.
- [32] S. D. Wright, R. A. Ramos, P. S. Tobias, R. J. Ulevitch, J. C. Mathison, *Science* **1990**, *249*, 1431.
- [33] M. Cuenca, J. Sintez, Á. Lányi, P. Engel, *Clin. Immunol. (Orlando, Fla.)* **2019**, *204*, 43.
- [34] L. Piccio, W. Vermi, K. S. Boles, A. Fuchs, C. A. Strader, F. Facchetti, M. Cella, M. Colonna, *Blood* **2005**, *105*, 2421.
- [35] M. B. Lutz, N. Kukutsch, A. L. Ogilvie, S. Rössner, F. Koch, N. Romani, G. Schuler, *J. Immunol. Meth.* **1999**, *223*, 77.
- [36] T. Buranda, J. Huang, G. V. Ramarao, L. K. Ista, R. S. Larson, T. L. Ward, L. A. Sklar, G. P. Lopez, *Langmuir* **2003**, *19*, 1654.